


 Cite this: *RSC Adv.*, 2021, 11, 34498

# Site-selective unidirectional benzylic $sp^3$ C–H oxidation of dodecahydrotriphenylene with $RuCl_3-NaIO_4$ : formation of benzylic ketones†‡

 Gaurang J. Bhatt,<sup>a</sup> Pradeep T. Deota,<sup>a\*</sup> Deepak Upadhyay<sup>b</sup> and Prafulla K. Jha<sup>c</sup>

 Received 24th May 2021  
 Accepted 1st October 2021

DOI: 10.1039/d1ra06897k

[rsc.li/rsc-advances](https://rsc.li/rsc-advances)

Dodecahydrotriphenylene, a higher homologue of trindane chemoselectively undergoes unidirectional benzylic  $sp^3$  C–H oxidation and the central benzene ring remains intact unlike that in trindane under similar reaction conditions.  $RuO_4$  which generally attacks  $sp^2$  C–H to form oxidative products is found to give benzylic ketones *via*  $sp^3$  C–H oxidation. Density functional theory (DFT) calculations have also been performed to analyse the potential energy, energy barrier and HOMO–LUMO energy gap of the products.

## Introduction

Selective transformation of benzocyclotrimers (BCTs) into their keto derivatives is highly desirable due to the diverse utility of the keto functionality in various synthetic elaborations towards graphene and buckminsterfullerene (Fig. 1). Hence, selective benzylic oxo-functionalization of alkylarenes is an important protocol in organic synthesis.<sup>1</sup> Moreover, benzylic oxidation of alkylarenes provides valuable synthons that can lead to many natural products, agrochemicals and pharmaceuticals.<sup>2</sup>

There are numerous reagents reported in the literature for selective benzylic oxo-functionalization such as  $NaClO/TEMPO/Co(OAc)_2$ , *o*-iodoxybenzoic acid,  $KMnO_4/MnO_2$ , bismuth-picolinic acid, *t*-BuONa, and ascorbic acid.<sup>3</sup> Ruthenium complexes have been commonly employed in various oxidative transformations to furnish a variety of oxo-functionalities.<sup>4–6</sup>

In general, Ru-compounds have been shown to attack alkenes *via*  $sp^2$  C–H activation to form aryl ketones.<sup>7</sup> However,  $RuCl_3-NaIO_4$  has been reported to exhibit poor reactivity during benzylic oxo-functionalization of alkylarenes *via*  $sp^3$  C–H activation.<sup>8a</sup> Hence, complexes of ruthenium have been employed to accomplish effective benzylic  $sp^3$  C–H oxidation of aromatic hydrocarbons to corresponding aromatic ketones.<sup>8b</sup>

Interestingly, the oxidation of tricyclopentabenzene (trindane, **1**) has been shown to yield a highly functionalized tricyclic system **2** (Scheme 1) upon oxidation with ruthenium tetroxide generated *in situ*.<sup>9</sup> It is remarkable to note that the compound **1** undergoes complete cleavage of the central benzene ring.

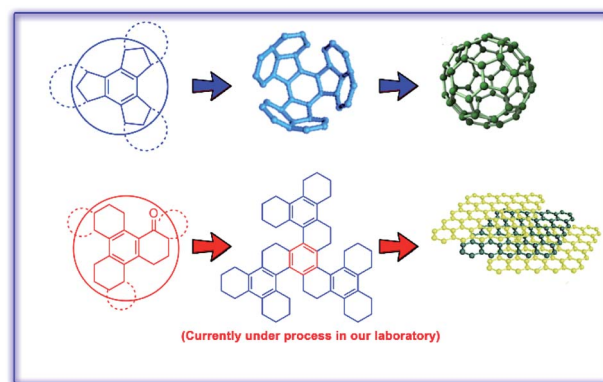


Fig. 1 Benzocyclotrimer precursors towards fullerene and graphene.

<sup>a</sup>Applied Chemistry Department, Faculty of Technology & Engineering, The Maharaja Sayajirao University of Baroda, Vadodara-390 001, Gujarat, India. E-mail: pteota-appchem@msubaroda.ac.in

<sup>b</sup>Department of Applied Physics, Faculty of Technology & Engineering, The Maharaja Sayajirao University of Baroda, Vadodara-390 001, Gujarat, India

<sup>c</sup>Department of Physics, Faculty of Science, The Maharaja Sayajirao University of Baroda, Vadodara-390 001, Gujarat, India

† The authors have dedicated this paper to Prof. Vishwakarma Singh on his 70<sup>th</sup> birthday.

‡ Electronic supplementary information (ESI) available. See DOI: 10.1039/d1ra06897k



In context with our synthetic studies, we became interested in examining the oxidation of dodecahydrotriphenylene **3** (readily assembled *via* cyclotrimerization of cyclohexanone), a higher homologue of compound **1**. Thus, we treated the compound **3** with  $\text{RuCl}_3\text{-NaIO}_4$  <sup>6</sup> in aqueous acetonitrile-carbon tetrachloride system at ambient temperature. The reaction was complete after 30 h (TLC). Usual workup and chromatography furnished the ketone **4** <sup>14</sup> along with hitherto unknown ketones **5** and **6** in a total yield of 37% (Scheme 2).

We undertook a time dependent study of the above oxidation by arresting the reaction at various intervals followed by work up and column chromatography of the reaction mixture. Initially, the reaction was done for 4 h during which formation of monoketone **4** was observed after 3 h, after which the formation of dione **5** (6%) was observed (TLC) (Table 1). The highest amounts of compound **5** (16%) was obtained when the reaction was conducted for 20 h. Similarly, the first appearance of trione **6** in trace amount was noticed after 16 h of the reaction which continued to rise and reached to a maximum when the reaction was done for 30 h (Table 1 and Fig. 2). The longer reaction time led to degradation of the products. In case of the entries 1–6, unreacted starting material was recovered.

The compound **3** does not undergo reaction when treated alone either with  $\text{RuCl}_3$  and/or  $\text{NaIO}_4$ . It was found that with lesser amounts of  $\text{NaIO}_4$  or  $\text{RuCl}_3$  or lesser reaction time, unreacted **3** was isolated. Attempts of benzylic oxidation of **3** using 18 equivalents of  $\text{NaIO}_4$  alone, in the absence  $\text{RuCl}_3$  met with no success. Similarly the reaction did not proceed without  $\text{NaIO}_4$  in the presence of  $\text{RuCl}_3$  alone indicating involvement of both the reagents in the oxidation cycle.

The structures of the dione **5** and trione **6** were deduced from their spectral features. Thus, the dione **5** exhibited a CO absorption band at  $1684\text{ cm}^{-1}$  in its IR spectrum which clearly indicated the presence of a conjugated carbonyl group. This suggested the presence of aromatic ring in compound **5**. The proton NMR spectrum (600 MHz) showed two signals at  $\delta$  3.29

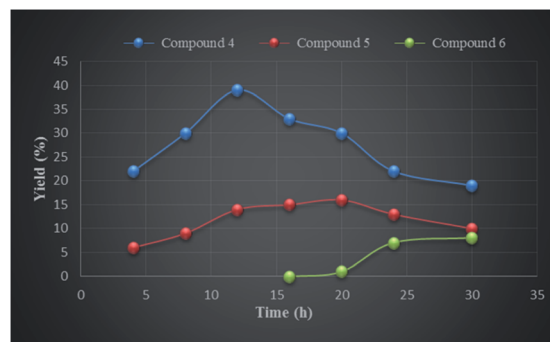


Fig. 2 Graphical presentation of the reaction time against yield (%) of compounds 4–6.

( $t, J = 6.0\text{ Hz}$ , 2H) and  $3.16$  ( $t, J = 6.2\text{ Hz}$ , 2H) due to methylene protons adjacent to carbonyl group. Further, signals were observed at  $\delta$  2.83 ( $q, J = 5.9\text{ Hz}$ , 3H), 2.63 ( $dt, J = 14.3, 6.1\text{ Hz}$ , 7H), 2.15–2.08 ( $m$ , 3H), 2.00–1.94 ( $m$ , 2H), 1.81 ( $dd, J = 11.5, 5.6\text{ Hz}$ , 2H) for other methylenes.  $^{13}\text{C}$  NMR (151 MHz,  $\text{CDCl}_3$ ) displayed signals at  $\delta$  200.98, 200.61 indicating the presence of conjugated carbonyl group. In addition, signals were seen at  $\delta$  148.11, 144.95, 134.33, 131.79 and 129.67, 40.71, 40.51, 30.36, 29.40, 29.18, 27.62, 27.47, 22.76, 22.61, 22.43, 22.27, 22.07.

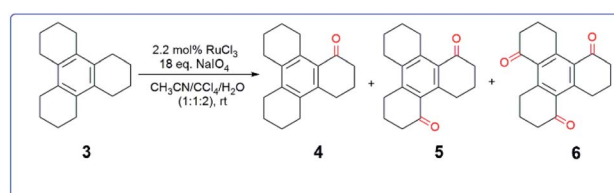
The trione **6** also exhibited a carbonyl absorption band at  $1690\text{ cm}^{-1}$  in its IR spectrum again indicating the presence of a conjugated carbonyl group. The proton NMR spectrum (600 MHz) of **6** showed only three sets of signals at  $\delta$  3.33 ( $t, J = 6.1\text{ Hz}$ , 1H) for methylenes adjacent to carbonyl, 2.68 ( $t, J = 6.8\text{ Hz}$ , 1H) for benzylic methylenes and 2.05–1.99 ( $m$ , 1H) for other methylene protons.  $^{13}\text{C}$  NMR (151 MHz,  $\text{CDCl}_3$ ) of **6** displayed only one signal at  $\delta$  200.12 indicating the presence of conjugated carbonyl groups. Further, only two signals for aromatic carbons were observed at  $\delta$  151.60, 131.79 and three signals in the aliphatic region at  $\delta$  40.32, 29.81 and 22.44. It is noteworthy to observe only six signals for eighteen carbons indicating  $C_{3v}$  symmetry in the molecule.

It is interesting to note that the above reaction furnished mono, di- and tri-keto derivatives in which the aromatic ring remains intact which is contrary to the behaviour of trindane **1** that undergoes complete oxidative cleavage of the aromatic ring.<sup>9</sup> Further, the structures of the dione **5** and trione **6** appear to have a unidirectional character in which the keto groups are present in either clockwise or anticlockwise direction. There are six benzylic positions available in compound **3** out of which only three positions are chemoselectively oxidized. None of the  $C_{2v}$  symmetric diones (**7–9**) were observed (Fig. 3). Consequently the

Table 1 Time-dependent study of the reaction

Entry <sup>a</sup>	Reaction time (h)	Yield <sup>b</sup> (%)		
		Compound <b>4</b>	Compound <b>5</b>	Compound <b>6</b>
1	04	22	6	—
2	08	30	9	—
3	12	39	14	—
4	16	33	15	Trace
5	20	30	16	Trace
6	24	22	13	7
7	30 <sup>c</sup>	<b>19</b>	<b>10</b>	<b>8</b>
8	72 <sup>d</sup>	—	—	—
9	96 <sup>e</sup>	NR	NR	NR

<sup>a</sup> Compound **3** (5.0 g) for each entry. <sup>b</sup> Isolated yields obtained after column chromatography. <sup>c</sup> Starting material **3** completely disappeared. <sup>d</sup> Complete degradation of reaction products observed. <sup>e</sup> No reaction (NR) either in presence of  $\text{RuCl}_3$  alone or  $\text{NaIO}_4$  alone and unreacted **3** was recovered.



Scheme 2 Formation of various benzylic ketones 4–6.



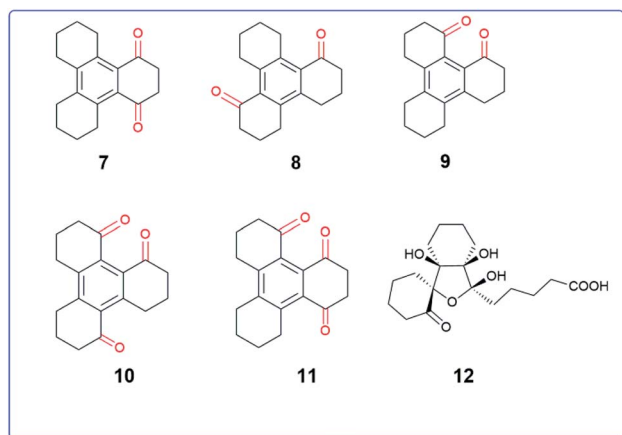


Fig. 3 Other possible benzylic diones, triones and the ring-opening product.

unsymmetrical triones **10** and **11** which could result from further oxidation of **7–9** were also not obtained.

It was also interesting to note that the oxidation did not give any ring-opened product of type **12** as expected from the report of S. Ranganathan *et al.*<sup>9</sup> It is known that ruthenium tetroxide is generated *in situ* using oxidants like periodate or hypochlorite.<sup>10</sup> The tetroxide thus formed experiences steric hindrance offered by the folded peripheral cyclohexene rings in compound **3**, which perhaps shield the attack of the oxidant on the central benzene ring (Fig. 4a and b) leading to consequent attack on the benzylic  $sp^3$  C–H positions.

$RuO_4$  is isoelectronic with  $OsO_4$  and due to its less toxicity, ruthenium is preferentially employed than osmium in oxidations.<sup>5b,6b</sup> A general mechanism for the oxidation is shown in Fig. 5. Initial benzylic hydrogen abstraction by *in situ* generated  $RuO_4$  (**7**) leads to formation of a corresponding free radical which on reaction with water gives an alcohol of type (**2**) forming Ru-oxo/hydroxo species (**3**).<sup>8a</sup> Further oxidation of (**2**) *via* intermediate (**4**) then leads to formation of a ketone (**5**) generating monooxoruthenium(IV) species (**6**) which is oxidized back to  $RuO_4$  (**7**) by the oxidant periodate for the next redox cycle.<sup>10</sup> Periodate itself gets reduced to iodate in the last step.

A comparison of various ruthenium assisted oxidations is presented in Scheme 3.  $\alpha$ -Diketones are obtained *via* ruthenium catalyzed  $sp^2$  C–H oxidation in which catalyst attacks the

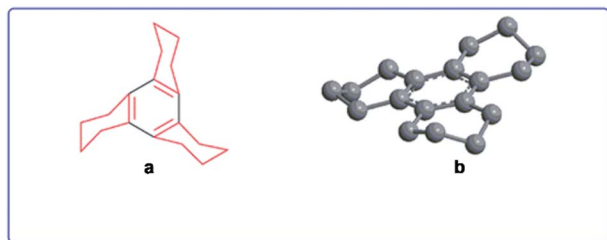


Fig. 4 (a) Folded peripheral cyclohexene rings around the central benzene ring in compound **3**. (b) Energy minimized structure of compound **3** by Chem3D.

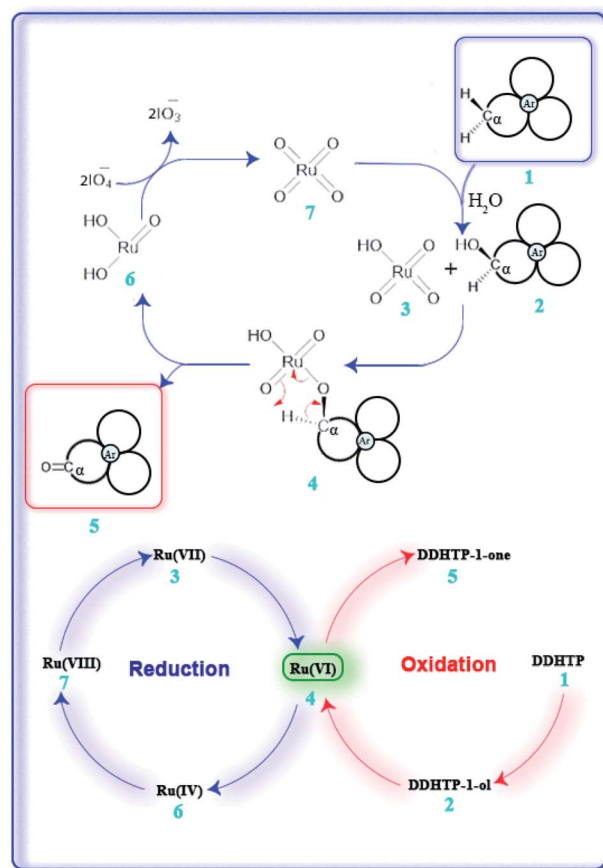


Fig. 5 Plausible mechanism of the ruthenium oxidation.

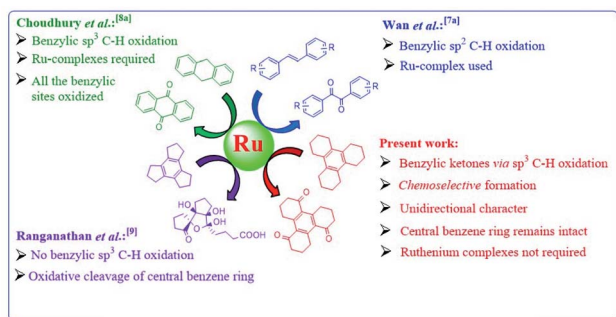
activated double bond of alkene.<sup>7a</sup> To achieve benzylic  $sp^3$  C–H oxidation, Ru-complexes have been employed.<sup>8a</sup> When  $Ru(VIII)$  species is used, trindane **1** undergoes complete oxidative cleavage of the central benzene ring to form polycyclic oxygenated product **2**.<sup>9</sup> Interestingly in spite of structural similarity between **1** and **3**,  $sp^3$  C–H oxidation is not observed in **1**. However we found that the central benzene ring in **3** remains intact and three out of six benzylic positions are chemoselectively oxidized to form a  $C_{3v}$  symmetric keto derivative **6** having unidirectional character along with **4** and **5** (Scheme 2).

### DFT calculations

We have performed independent structural optimization of all the possible isomers of diones and triones to determine their minimum energy. Further calculations such as ground-state structural and electronic (HOMO–LUMO) were performed using density functional theory based on first principle calculations using the Gaussian09 suite of program.<sup>11</sup>

The Becke three parameters hybrid functional with Lee–Yang–Perdew correlation functionals (B3LYP)<sup>12</sup> are utilized with LanL2DZ basis-set for the Ru-based systems and 6-311G basis-set for rest the systems to accurately predict the minimum energy states. The hybrid functionals are the mixture of Hartree–Fock (HF) exchange along with density functional theory (DFT) exchange–correlation functionals. B3LYP functional uses





Scheme 3 An overview of ruthenium mediated oxidations.

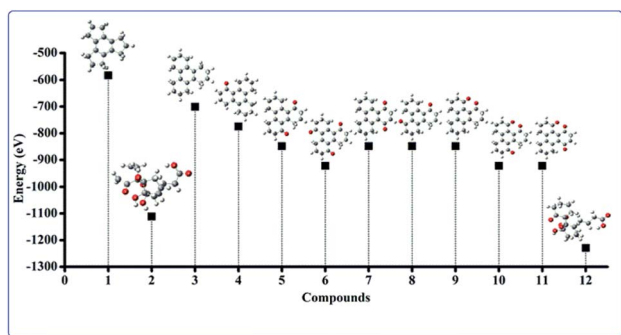


Fig. 6 Optimized geometries of the molecules corresponding to their energy state.

LYP expression for non-local correlation and VWN function III for local correlation. The optimized structures were visualized using GaussView (version 5).<sup>13</sup> The HOMO–LUMO gap is also evaluated as it gives the important parameters such as electronegativity ( $\chi$ ), chemical potential ( $\mu$ ), global hardness ( $\eta$ ), global electrophilicity index ( $\omega$ ) and global softness ( $S$ ) etc.

In order to validate the experimental findings and to understand the atomic level properties we have individually configured and optimized the structural geometries by utilizing the parameters described above. The optimized geometries along with the energies are presented in the Fig. 6. It can be observed that the minimum energies are obtained for the compounds 4, 5 and 6 that can also be observed in experimental results.

Fig. 6 shows the optimized geometry calculated using the DFT method that corresponds to the energy of the molecules. The calculated potential energy of compounds 4, 5 and 6 are  $-774.392$  eV,  $-848.401$  eV and  $-922.410$  eV respectively. Compounds 5 and 6 have lower minimized energy than their corresponding possible diones [7 ( $-848.398$  eV), 8 ( $-848.398$  eV) and 9 ( $-848.398$  eV)] and triones [10 ( $-922.401$  eV), 11 ( $-922.401$  eV)] respectively.

$Ru(VIII)$  is the most stable state among its other prevalent oxidation states. The continuous reduction from  $Ru(VIII)$  via ruthenate(VI) as an intermediate state leads to the formation of most common  $Ru(IV)$  oxidation state. We have calculated relative energy pathway and energy barrier for each step and plotted

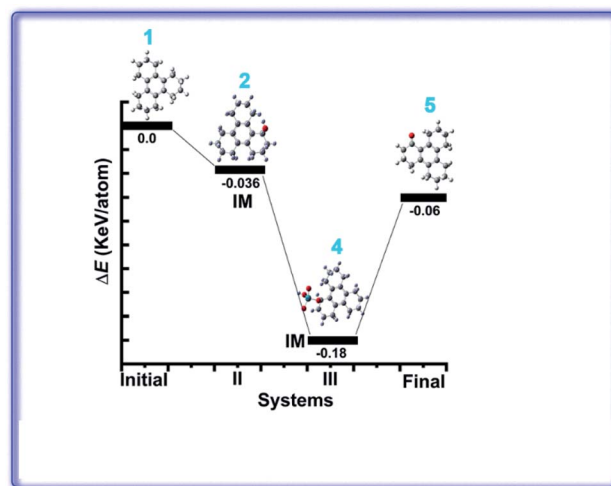


Fig. 7 Calculated relative energy pathway of the intermediates (IM) during oxidation reaction.

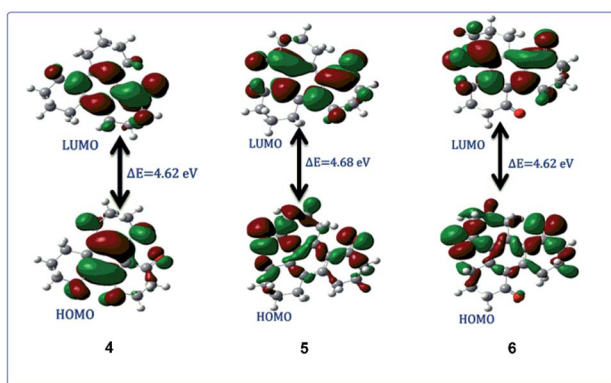


Fig. 8 The HOMO–LUMO gap of compounds 4, 5 and 6.

the energy diagram (Fig. 7). Initially  $RuO_4$  abstracts a hydrogen from 3, leading to its reduction into  $Ru(VII)$  with concomitant formation of the hydroxy derivative (IM-2). The calculated energy barrier for this step is  $-0.036$  keV per atom. This is followed by the combination of IM-2 and  $Ru(VII)$  species giving rise to the alkoxyruthenium(VI) (IM-4) having  $-0.144$  keV per atom energy barrier for this step. In the key step, ruthenium–oxygen bond cleavage leads the formation of the keto-products along with the generation of  $Ru(IV)$ . The energy barrier for this last step is  $0.12$  keV per atom. The calculated HOMO–LUMO energy gap of 4, 5 and 6 are shown in the Fig. 8.

## Conclusions

In summary, the central benzene ring of compound 3 is found to remain unaffected by ruthenium and subsequently  $sp^3$  C–H benzylic oxidation leading to formation of benzylic ketones 4–6 is observed. The DFT calculations reflect strong agreement with our experimental data. Further investigations on scope of these ketones are currently under process in our laboratory.



## Conflicts of interest

There are no conflicts to declare.

## Acknowledgements

GB acknowledges award of a research fellowship under DST-PURSE program. Authors thank M/s Hindustan Platinum Pvt. Ltd, Navi Mumbai & Ravindra Heraeus Pvt Ltd, Jaipur for providing gift samples of RuCl<sub>3</sub>.

## Notes and references

- (a) D. Alberico, M. E. Scott and M. Lautens, *Chem. Rev.*, 2007, **107**, 174–238; (b) E. M. Beccalli, G. Broggini, M. Martinelli and S. Sottocornola, *Chem. Rev.*, 2007, **107**, 5318–5365; (c) X. Chen, K. M. Engle, D.-H. Wang and J.-Q. Yu, *Angew. Chem., Int. Ed.*, 2009, **48**, 5094–5115; (d) R. Giri, B.-F. Shi, K. M. Engle, N. Maugel and J.-Q. Yu, *Chem. Soc. Rev.*, 2009, **38**, 3242–3272; (e) R. Jazzar, J. Hitce, A. Renaudat, J. Sofack-Kreutzer and O. Baudoin, *Chem.–Eur. J.*, 2010, **16**, 2654–2672; (f) T. W. Lyons and M. S. Sanford, *Chem. Rev.*, 2010, **110**, 1147–1169; (g) R. A. Sheldon and J. K. Kochi, in *Advances in Catalysis*, ed. D. D. Eley, H. Pines and P. B. Weisz, Academic Press, 1976, vol. 25, pp. 272–413; (h) C. Guo, D. Xia, Y. Yang and X. Zuo, *Chem. Rec.*, 2019, **19**, 2143–2156.
- H. Hussain, I. R. Green and I. Ahmed, *Chem. Rev.*, 2013, **113**, 3329–3371.
- (a) Y. Bonvin, E. Callens, I. Larrosa, D. A. Henderson, J. Oldham, A. J. Burton and A. G. M. Barrett, *Org. Lett.*, 2005, **7**, 4549–4552; (b) C. Jin, L. Zhang and W. Su, *Synlett*, 2011, **2011**, 1435–1438; (c) J.-S. Li, F. Yang, Q. Yang, Z.-W. Li, G.-Q. Chen, Y.-D. Da, P.-M. Huang, C. Chen, Y. Zhang and L.-Z. Huang, *Synlett*, 2017, **28**, 994–998; (d) K.-J. Liu, Z. Wang, L.-H. Lu, J.-Y. Chen, F. Zeng, Y.-W. Lin, Z. Cao, X. Yu and W.-M. He, *Green Chem.*, 2021, **23**, 496; (e) K. J. Liu, T. Y. Zeng, J. L. Zeng, S. F. Gong, J. Y. He, Y. W. Lin, J. X. Tan, Z. Cao and W. M. He, *Chin. Chem. Lett.*, 2019, **30**, 2304–2308; (f) F.-L. Zeng, X.-L. Chen, S.-Q. He, K. Sun, Y. Liu, R. Fu, L.-B. Qu, Y.-F. Zhao and B. Yu, *Org. Chem. Front.*, 2019, **6**, 1476–1480; (g) W.-B. He, L.-Q. Gao, X.-J. Chen, Z.-L. Wu, Y. Huang, Z. Cao, X.-H. Xu and W.-M. He, *Chin. Chem. Lett.*, 2020, **31**, 1895–1898.
- (a) S. Funyu, T. Isobe, S. Takagi, D. A. Tryk and H. Inoue, *J. Am. Chem. Soc.*, 2003, **125**, 5734–5740; (b) O. Nestler and K. Severin, *Org. Lett.*, 2001, **3**, 3907–3909; (c) M. K. Tse, M. Klawonn, S. Bhor, C. Döbler, G. Anilkumar, H. Hugl, W. Mägerlein and M. Beller, *Org. Lett.*, 2005, **7**, 987–990; (d) W.-P. Yip, W.-Y. Yu, N. Zhu and C.-M. Che, *J. Am. Chem. Soc.*, 2005, **127**, 14239–14249; (e) X.-Q. Yu, J.-S. Huang, W.-Y. Yu and C.-M. Che, *J. Am. Chem. Soc.*, 2000, **122**, 5337–5342; (f) J.-L. Zhang, H.-B. Zhou, J.-S. Huang and C.-M. Che, *Chem.–Eur. J.*, 2002, **8**, 1554–1562.
- (a) C.-M. Ho, W.-Y. Yu and C.-M. Che, *Angew. Chem., Int. Ed.*, 2004, **43**, 3303–3307; (b) B. Plietker and M. Niggemann, *Org. Lett.*, 2003, **5**, 3353–3356; (c) T. K. M. Shing, V. W.-F. Tai and E. K. W. Tam, *Angew. Chem., Int. Ed.*, 1994, **33**, 2312–2313; (d) T. K. M. Shing and E. K. W. Tam, *Tetrahedron Lett.*, 1999, **40**, 2179–2180; (e) T. K. M. Shing, E. K. W. Tam, V. W.-F. Tai, I. H. F. Chung and Q. Jiang, *Chem.–Eur. J.*, 1996, **2**, 50–57; (f) R. Zhang, W.-Y. Yu, K.-Y. Wong and C.-M. Che, *J. Org. Chem.*, 2001, **66**, 8145–8153.
- (a) P. H. J. Carlsen, T. Katsuki, V. S. Martin and K. B. Sharpless, *J. Org. Chem.*, 1981, **46**, 3936–3938; (b) B. Plietker, *J. Org. Chem.*, 2003, **68**, 7123–7125; (c) F. Sondheimer, R. Mechoulam and M. Sprecher, *Tetrahedron*, 1964, **20**, 2473–2485; (d) G. Stork, A. Meisels and J. E. Davies, *J. Am. Chem. Soc.*, 1963, **85**, 3419–3425; (e) S. Wolfe, S. K. Hasan and J. R. Campbell, *J. Chem. Soc. D*, 1970, 1420–1421, DOI: 10.1039/C29700001420; (f) D. Yang and C. Zhang, *J. Org. Chem.*, 2001, **66**, 4814–4818.
- (a) S. Chen, Z. Liu, E. Shi, L. Chen, W. Wei, H. Li, Y. Cheng and X. Wan, *Org. Lett.*, 2011, **13**, 2274–2277; (b) J. Hu, D. Zhang and F. W. Harris, *J. Org. Chem.*, 2005, **70**, 707–708.
- (a) S. K. Gupta and J. Choudhury, *ChemCatChem*, 2017, **9**, 1979–1984; (b) C. S. Yi, K.-H. Kwon and D. W. Lee, *Org. Lett.*, 2009, **11**, 1567–1569.
- S. Ranganathan, K. M. Muraleedharan, P. Bharadwaj and K. P. Madhusudanan, *Chem. Commun.*, 1998, 2239–2240.
- I. W. C. E. Arends, T. Kodama and R. A. Sheldon, in *Ruthenium Catalysts and Fine Chemistry*, Berlin, Heidelberg, 2004, pp. 277–320.
- M. Caricato, Æ. Frisch, J. Hiscocks and M. J. Frisch, *Gaussian 09: I/Ops Reference*, Gaussian, Inc, Wallingford, CT 06492, U.S.A., 2nd edn, 2009.
- A. D. Becke, *Phys. Rev. A*, 1986, **33**, 2786–2788.
- A. Frisch, A. B. Nelson and A. J. Holder, *Gaussview*, Pittsburgh, Pa, USA, 2005.
- M. Farina and G. Audisio, *Tetrahedron*, 1970, **26**, 1827–1837.

